The South Indian Ocean Current

LOTHAR STRAMMA

Institut für Meereskunde an der Universität Kiel, Kiel, Federal Republic of Germany

4 March 1991 and 23 July 1991

ABSTRACT

In this paper, the historical hydrographic database for the south Indian Ocean is used to investigate (i) the hydrographic boundary between the subtropical gyre and the Antarctic Circumpolar Current (ACC), the subtropical front (STF), and especially (ii) the southern current band of the gyre. A current band of increased zonal speeds in the upper 1000 m is found just north of the STF in the west near South Africa and at the surface STF in the open Indian Ocean until the waters off the coast of Australia are reached. As neither any other investigation of this current nor a name for it are known, the flow has been called the South Indian Ocean Current (SIOC). This name is anologous to the same current band in the South Atlantic Ocean, the South Atlantic Current. The STF is located in the entire south Indian Ocean near 40°S. The associated current band of increased zonal speeds is the SIOC, which is found at or north of the STF. East of 100°E the SIOC separates from the STF and continues to the northeast. The zonal flow south of the STF is normally weak and serves to separate the South Indian Ocean and Circumpolar currents. Near Africa the SIOC has a typical volume transport of 60 Sv (1 Sv $\equiv 10^6$ m^3 s^{-1}) in the upper 1000 m relative to deep potential density surfaces of σ_4 = 45.87 kg m^{-3} (2800–3500 m) or σ_2 = 36.94 kg m^{-3} (1500–2500 m). Near western Australia the SIOC is reduced to about 10 Sv as it turns to the northeast.

1. Introduction

For the South Atlantic Ocean, Stramma and Peterson (1990) were able to show that a current band called the South Atlantic Current (SAC) exists at the subtropical front (STF) at about 40°S, which is the southern current of the South Atlantic subtropical gyre and is separated from the circumpolar currents by a zone of relatively weak flow. The SAC was found at or north of the surface STF and extends eastward until Indian Ocean water from the Agulhas retroflection is encountered. A reversal of baroclinicity in the STF was observed south of a highly saline Agulhas ring, causing the SAC to separate from the STF and turn north into the Benguela Current.

In the Indian Ocean south of Africa, the water from the Agulhas retroflection flows eastward and is called the Agulhas Return Current (AGR). It seems worthwhile looking into the eastward extension of the AGR and investigating whether a current band distinct from the circumpolar currents also exists in the southern Indian Ocean. Peterson and Stramma (1991, their Fig. 8) showed a schematic representation of the Agulhas Current system adapted from investigations by Lutjeharms and Van Ballegooyen (1988) and Lutjeharms (1989). It shows the Agulhas Return Current as well as the subtropical front at about 40°S in the southwestern Indian Ocean. Bennett (1988) computed the Agulhas Return Current transport for two sections as 54 and 65 Sv (1 Sv $\equiv 10^6$ m^3 s^{-1}).

The hydrographic boundary in the South Atlantic between the subtropical gyre and the Antarctic Circumpolar Current (ACC) was described by Deacon (1933) as the subtropical convergence. According to Deacon (1933, pp. 210 and 216) the convergence "is marked by a sudden change of surface temperature of at least 4°C, and a change of salinity of at least 0.50." In a more comprehensive paper, Deacon (1937, p. 72) stated, "the water just north of the convergence has a temperature of at least 11.5°C in winter and 14.5°C in summer, but where there is a strong southward movement the temperature may be as much as 5°C higher, . . . the salinity of the surface water is at least 34.9, and it may be as much as 35.5."

To the south of western Australia the subtropical convergence was first observed by Deacon (1937) to be near 40°S. Deacon (1937) showed in his Fig. 4 the subtropical convergence to be a continuous feature from the Brazil–Falkland confluence area in the Atlantic through the Indian Ocean to New Zealand, and from New Zealand into the central Pacific. A schematic representation of the STF (called subtropical convergence) in the Indian Ocean is given also by Tchernia (1980, his Fig. 6.1). It shows the STF just south of 40°S in most areas except near 80° and 110°E, where the front is shown just north of 40°S. The southernmost extent of the STF is presented for Tasmania,

Corresponding author address: Dr. Lothar Stramma, Institut für Meereskunde, Düsternbrooker Weg 20, 2300 Kiel, Federal Republic of Germany.

where the front is located just south of Tasmania at about 45°S.

More intense investigations of the STF near Australia were done by Cresswell et al. (1978) and Edwards and Emery (1982). Cresswell et al. (1978) investigated the eddying behavior of a satellite-tracked buoy near the subtropical convergence zone southwest of Australia at 112°–118°E. Surface salinity and temperature plots revealed spatial variations characteristic of subtropical convergence as well as an intrusion of warm highly saline water from the north, showing the STF between 38° and 40°S. Edwards and Emery (1982) used 14 north–south XBT sections to define the positions of different fronts south of Australia. According to their results the STF is always south of 40°S between 95°E and 170°W.

In this paper, we use hydrographic measurements from a number of cruises to investigate the course of the STF across the south Indian Ocean and to compute the zonal velocities and transports of the associated current. This zonal current is distinct from the ACC and closes the upper-level circulation of the subtropical gyre in the south. In accordance with the analogous current in the South Atlantic, the South Atlantic Current, we call this current the South Indian Ocean Current (SIOC). The currents south of South Africa are quite well investigated, mainly by South African scientists, and transport values are known; therefore, we restrict the investigation to the much less described region east of 30°E.

2. Methods

Several quasi-synoptic hydrographic sections from the period 1934 to 1974 crossing the STF or sections near to it in the south Indian Ocean plus two zonal sections near the west Australian coast (Fig. 1) have been extracted from a digitized database supplied by the World Oceanographic Data Center (WODC) in Washington, D.C. Some basic details concerning the sections are provided in Table 1, together with the locations of the stations immediately north and south of the STF and their surface salinities and temperatures. The two zonal sections near Australia (not listed in Table 1) were done by R/V *Diamantina* in February 1960 and by R/V *Vityaz* in December 1959. Although each cruise in itself was quasi-synoptic, the dataset from 1934 to 1974 is a quite inhomogeneous collection. For sure, there must have been meridional sections made after 1974, but they were still not contained in the WODC dataset available to us; the meridional sections used here are the complete set of meridional sections from this dataset and not a subset.

In the following, the STF is identified on the basis of maximum near-surface salinity and temperature gradients loosely following Deacon (1933, 1937). The higher priority was put on the salinity front, as the temperature signal varies more with the season.

For geostrophic computations, a variable reference depth based on water mass properties is assumed. A summary of the major water masses in the Indian Ocean is given by Wyrtki (1971). Below the South Indian Central Water (SICW) in the upper ocean north of the STF, the Antarctic Intermediate Water (AAIW), indicated by a salinity minimum and an oxygen maximum, spreads northward to about 10°S. Below the AAIW an oxygen minimum is found, which Wyrtki (1971) showed to be at the density $\sigma_0 = 27.6$ kg m^{-3} between 30° and 50°S. Underneath that oxygen minimum the deep water is located, which is called Atlantic–Indian Deep Water by Dietrich et al. (1980), Common Water by Montgomery (1958), or Circumpolar Deep Water by Emery and Meincke (1986).

In the southwestern Indian Ocean the deep water shows a salinity maximum at about 2500 m and is clearly due to the North Atlantic Deep Water being carried eastward (Warren 1981). The figure of steric height at 2000–3500 db (Reid 1981) shows also that this layer carries water eastward at about 40°S.

Therefore, the best choice for a reference layer of

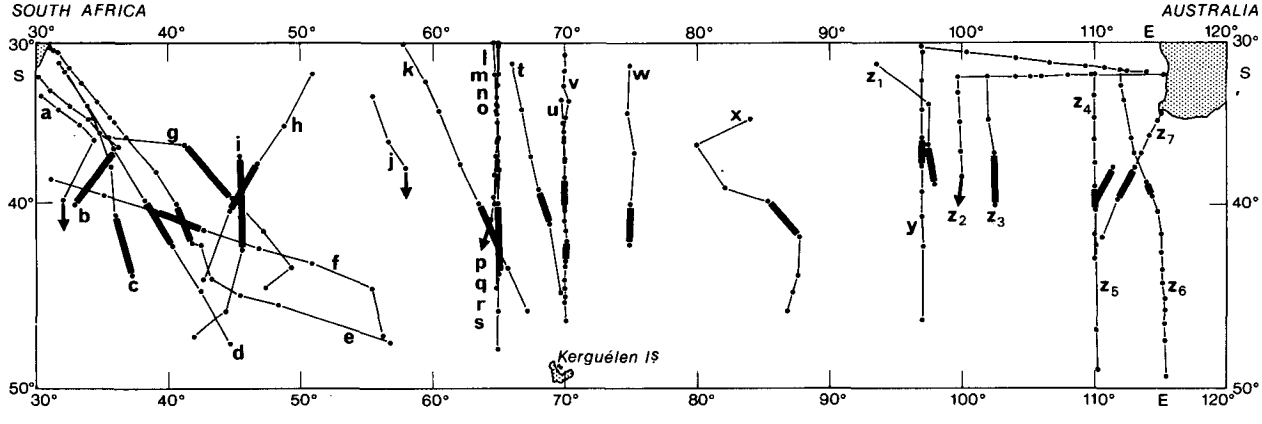

FIG. 1. The sections (lines) and positions (dots) of hydrographic stations used. Letters correspond to cruises listed in Table 1. Heavy bars indicate positions of the subtropical front, arrows indicate the front to be located south of the southernmost station.

TABLE 1. Sections appearing in Fig. 1 together with positions of the stations to the immediate north and south of the subtropical front (STF) and their surface salinities and temperatures.

	Ship	Longitude	Time	STF location	Surface salinity (psu)	Surface temperature (°C)
(a)	*Natal*	30°–34°E	Aug 1962	s of 39.8°S, 32.0°E	—	—
(b)	*Natal*	30°–36°E	Oct 1962	36.6°–40.1°S, 34.0°E	35.2–35.6	13.4–17.9
(c)	*Discovery*	32°–37°E	Apr 1935	40.7°–44.1°S, 37.0°E	33.9–35.3	8.0–15.5
(d)	*Discovery*	31°–45°E	May 1934	39.8°–42.4°S, 39.0°E	33.9–35.2	8.7–15.3
(e)	*Conrad*	31°–57°E	Apr 1974	40.0°–42.3°S, 41.0°E	34.2–36.3	12.7–19.0
(f)	*Discovery*	31°–56°E	Nov 1935	40.5°–41.5°S, 41.0°E	34.3–35.4	9.6–15.1
(g)	*Africana*	35°–47°E	Jul 1962	36.5°–39.7°S, 43.0°E	35.0–35.6	13.2–17.8*
(h)	*Fuji*	42°–51°E	Mar 1970	37.6°–40.3°S, 45.5°E	35.1–35.5	16.0–19.7
(i)	*Vema*	42°–46°E	Jan 1960	37.1°–42.6°S, 45.5°E	34.9–35.2	14.4–18.4
(j)	*Africana*	55°–58°E	Jul 1961	s of 37.9°S, 58.0°E	—	—
(k)	*Unknown F*	58°–67°E	Jan 1956	40.0°–42.0°S, 64.0°E	35.1–35.4	13.9–15.5
(l)	*Korolev*	64°–65°E	Feb 1973	s of 39.6°S, 64.8°E	—	—
(m)	*Korolev*	64°–65°E	Mar 1973	s of 40.0°S, 64.8°E	—	—
(n)	*Anton Bruun*	64°–65°E	Jul 1964	s of 41.0°S, 64.5°E	—	—
(o)	*Schokalsky*	65°E	Feb 1970	42.0°–44.0°S, 65.0°E	34.2–35.2	11.8–16.0
(p)	*Schokalsky*	65°E	Jul 1970a	40.0°–42.0°S, 65.0°E	34.9–35.2	12.1–13.3
(q)	*Schokalsky*	65°E	Jul 1970b	42.0°–44.0°S, 65.0°E	33.8–35.2	5.8–13.3
(r)	*Voeikov*	65°E	Jan 1969	40.0°–42.0°S, 65.0°E	34.8–35.6	13.7–15.2
(s)	*Voeikov*	65°E	Apr 1970	s of 40.0°S, 65.0°E	—	—
(t)	*Ob*	66°–70°E	May 1956	39.2°–41.2°S, 68.0°E	34.8–35.2	13.4–14.9
(u)	*Shirshov*	70°E	Mar 1975	38.7°–40.3°S, 70.0°E	34.7–35.3	14.9–17.9*
(v)	*Shirshov*	70°E	Nov 1970	42.1°–43.3°S, 70.0°E	34.4–35.2	9.8–13.0†
(w)	*Anton Bruun*	75°E	Apr 1964	40.1°–42.3°S, 75.0°E	34.7–35.2	12.1–15.0
(x)	*Eltanin*	80°–88°E	Composite	39.9°–42.0°S, 86.0°E	34.8–35.0	10.7–11.8
(y)	*Ob*	97°E	Apr 1957	36.1°–37.8°S, 97.0°E	34.9–35.4	13.8–16.4
(z1)	*Eltanin*	93°–98°E	Jul 1971	36.5°–38.9°S, 97.5°E	34.8–35.1	10.9–12.9
(z2)	*Diamantina*	100°E	Feb 1960	s of 38.3°S, 100.0°E	—	—
(z3)	*Diamantina*	102°E	Feb 1960	37.0°–40.2°S, 102.0°E	34.9–35.8	14.4–18.5
(z4)	*Diamantina*	110°E	Sep 1962	39.0°–40.5°S, 110.0°E	34.9–35.4	10.4–13.4
(z5)	*Eltanin*	110°–111°E	Sep 1962	37.9°–40.0°S, 110.5°E	34.9–35.3	10.6–12.4
(z6)	*Voekov*	112°–115°E	Nov 1970	38.7°–39.6°S, 114.0°E	34.7–35.4	11.7–14.3
(z7)	*Ob*	110°–115°E	Feb 1970	37.9°–39.8°S, 112.0°E	34.9–35.4	15.4–17.8

* Secondary temperature and salinity fronts to the south.
† Secondary salinity front to the north.

low zonal flow would lie underneath the deep water and above the Antarctic Bottom Water, which spreads northward. We have choosen the density $\sigma_4 = 45.87$ kg m^{-3}, which is located between these two water masses, as the reference surface. This density generally lies in the depth range of 2800–3500 m and is computed using the IES-80 density equation. Since the stations in the central and eastern south Indian Ocean often did not reach that depth, a density surface below the oxygen minimum at $\sigma_0 = 27.6$ kg m^{-3} below the AAIW was chosen as an alternative. From the different sections a density surface of $\sigma_2 = 36.94$ kg m^{-3} (near $\sigma_0 = 27.75$ kg m^{-3}) turned out to be the best choice of a density surface between the layer of the oxygen minimum and the deep water lying underneath. This density surface lies in the depth range of 1500–2500 m. The current crosses the Southwest Indian Ridge near 40°S, 50°E with water depths of less than 2000 m. Since this ridge blocks the deep water flow, the reference level of $\sigma_2 = 36.94$ kg m^{-3} will be a reasonable reference layer east of 50°E.

In their investigation of the Benguela Current, Stramma and Peterson (1989) also found the density of $\sigma_0 = 27.75$ kg m^{-3} to be the best choice of a layer between the upper branch of Circumpolar Deep Water and the underlying North Atlantic Deep Water. The location of the two density surfaces chosen here in relation to the temperature, salinity, and oxygen distribution, as well as the computed geostrophic speed, can be seen in Figs. 2 and 3. For stations not even reaching the shallower density surface, the lowest common depth of two stations is used in order to get at least some information about the transport, although these values will underestimate the total transport.

3. Observations

a. The STF in the Indian Ocean

The two sections of Figs. 2 and 3 represent the parameter distribution in the west and in the east of the south Indian Ocean across the STF. In the west, the

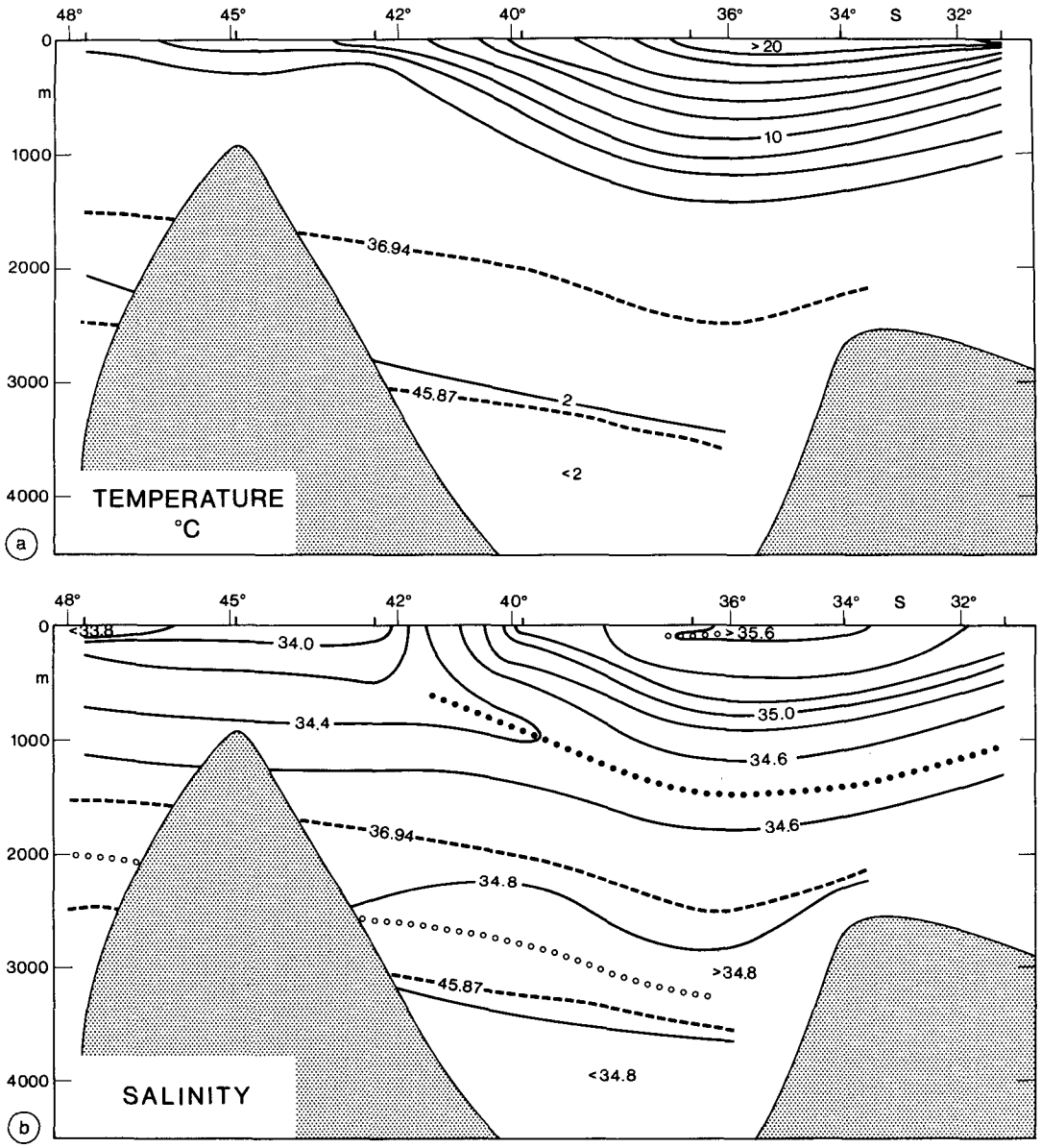

FIG. 2. Vertical distribution of (a) temperature in degrees celcius, (b) salinity, (c) oxygen in milliliters per liter, and (d) northeastward geostrophic speed in centimeters per second (southwestward speed is shaded) relative to the potential density surface σ_4 = 45.87 kg m^{-3} along the southeast (left)–northwest (right) line of stations occupied by R/V *Discovery* at 45°–31°E. Relative maxima are denoted by open circles and minima by dots. Also shown are the isopycnals of σ_2 = 36.94 kg m^{-3} and σ_4 = 45.87 kg m^{-3} (broken line).

R/V *Discovery* section at 31°–44°E (section d in Fig. 1) is used as an example in Fig. 2 to show the vertical distribution of temperature, salinity, and oxygen and the eastward geostrophic velocity. Strong surface salinity, temperature, and oxygen gradients appear between 39.8° and 42.4°S, clearly indicating the STF. These strong gradients are also present in the top 1000 m of the water column. In the oxygen field, the contrast between upper-level water masses is clear. North of about 40°S is a lens of poorly oxygenated (<5 ml l^{-1}) near-surface water typical of the subtropics (here the South Indian Central Water), whereas to the south oxygen-rich surface waters are present belonging to the Subantarctic Zone (SAZ). The oxygen maximum of the AAIW lies at about 300–650 m north of the STF, while the salinity minimum of the AAIW is found at greater depths of 600–1300 m. Underneath this minimum the oxygen minimum is located near the depth σ_0 = 27.6 kg m^{-3}. The salinity maximum of the deep water is found here at about 2000 m in the south of the *Dis-*

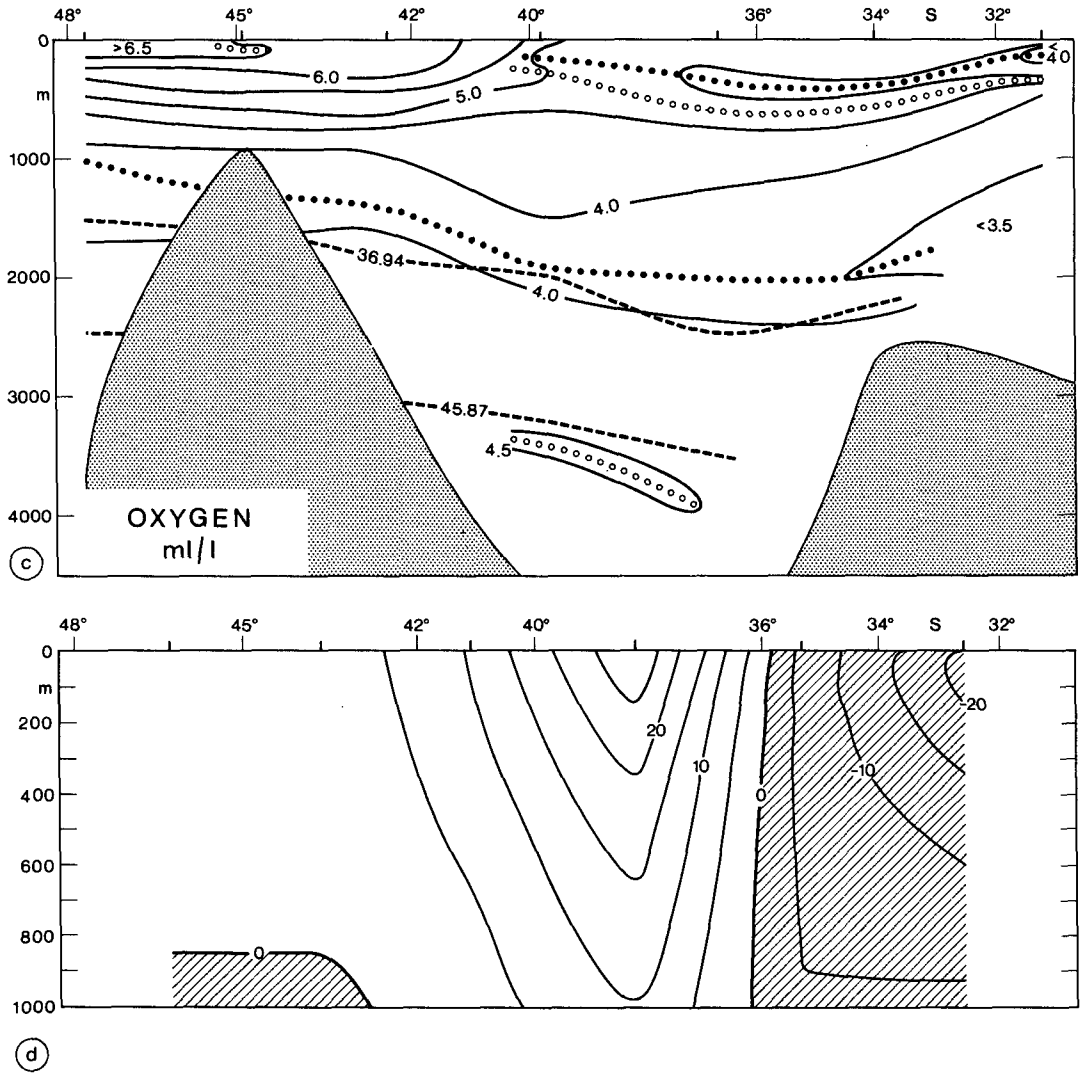

FIG. 2. (*Continued*)

covery section (Fig. 2) and near 3000 m underneath the subtropical gyre. As can be seen, the two density surfaces used here as reference levels are above and below the deep water. The velocity distribution clearly shows a strong current band north of the STF, while to the south of the front the velocities in the upper 1000 m are weak.

The section in the east of the southern subtropical Indian Ocean (Fig. 3) was done by R/V *Diamantina* at 110°E (section z4 in Fig. 1). A clear surface salinity front is seen at 39.0°–40.5°S and is accompanied by less pronounced surface temperature and oxygen fronts, indicating the STF. These gradients are not so strong as in the west (Fig. 2) and also do not reach that far down. The water mass distribution and the parameter extrema, as described for Fig. 2, are also valid for the *Diamantina* section (Fig. 3). The oxygen field for the South Indian Central Water is not so poorly oxygenated as in the west. The unexpected result is that the transport at the front at 110°E (Fig. 3) is not to the east as at the STF in all sections west of 90°E but rather to the west.

The front location of the other sections shown in Fig. 1 are listed in Table 1 and are marked also in Fig. 1 by the heavy lines. According to Table 1 the STF is near or south of 40°S in the southwestern Indian Ocean and at or north of 40°S in the southeast. This is in agreement with the older literature. The STF might also shift with time, as can be seen from the different sections at 65° or at 70°E.

b. Course of the STF and transport of the SIOC

The geostrophic velocity distribution and transport rates for all sections used were computed and are shown in Table 2. Except for the southeastern Indian Ocean

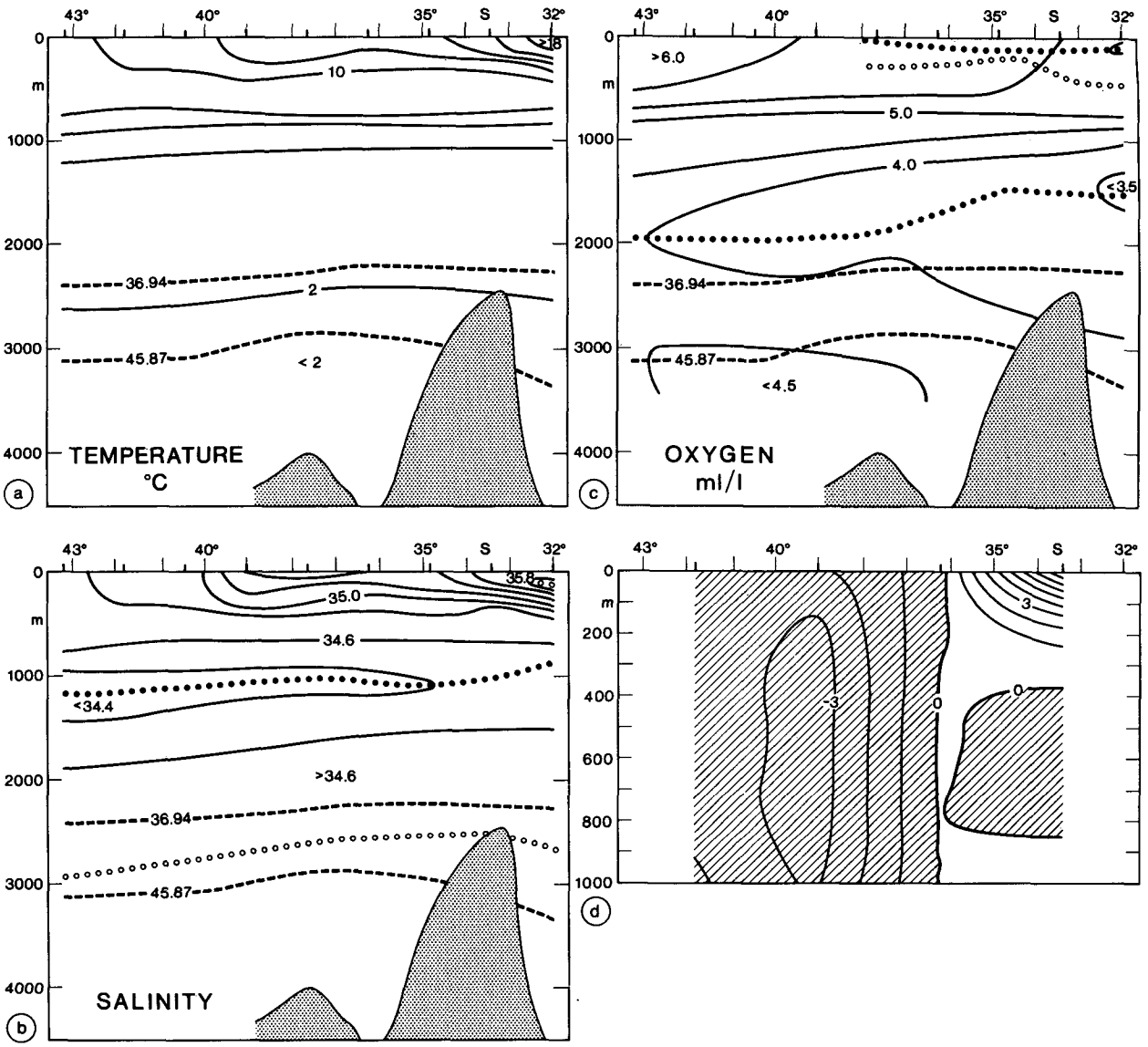

FIG. 3. Vertical distribution of (a) temperature in degrees celcius, (b) salinity, (c) oxygen in milliliters per liter, and (d) eastward geostrophic speed in centimeters per second (westward speed is shaded) relative to the potential density surface σ_4 = 45.87 kg m^{-3} along the south (left)–north (right) line of stations occupied by R/V *Diamantina* at 110°E. Relative maxima are denoted by open circles and minima by dots. Also shown are the isopycnals of σ_2 = 36.94 kg m^{-3} and σ_4 = 45.87 kg m^{-3} (broken line).

near Australia, a current band is observed just north of the STF in the west near South Africa and at the STF in the open Indian Ocean. The example in Fig. 2 shows the core of the current band to the north of the STF with a maximum surface velocity of 29.2 cm s^{-1}. But even at 1000-m depth, the current speed is still almost 10 cm s^{-1}. The surface velocities (Table 2) are up to 33 cm s^{-1}, but due to the generally large station spacing the real velocities are underestimated and the values of Table 2 represent only the mean over the distance between two stations. Findlay (1866) described the movement of a current bottle that moved with a mean velocity of 9.1 m day^{-1} (=19 cm s^{-1}) from 39°39′S, 66°07′E to Australia. This very early observation of strong eastward flow near 40°S is comparable to the surface velocities computed here.

In several sections (Table 2), westward transports of the upper 1000 m are found north of the STF. The transport values in Table 2 north of the front are given in order to compare the flow at the front with the flow north of it, but the numbers need some explanation. At section (b) (R/V *Natal*), the 11.8 Sv westward are compensated by 12.0 Sv flowing eastward by the next two station pairs to the north of the westward flow. As in Table 2 the transport north of the STF is computed only until a reversal in flow direction is encountered,

TABLE 2. Depths of the potential density surface of σ_4 = 45.87 kg m^{-3} (marked by @) or σ_2 = 36.94 kg m^{-3} used as reference for geostrophic calculations, together with maximum eastward geostrophic speeds at the surface for the South Indian Ocean Current (SIOC) and eastward geostrophic transports (1 Sv ≡ 10^6 m^3 s^{-1}) in the upper 1000 m for the station pairs spanning the subtropical front (STF, shown as heavy bars in Fig. 1). Transport values for regions north of the STF are computed from the front northward to either the end of the particular section or until reversal in flow direction is encountered. The final column gives transport values for station pairs immediately south of the STF.

Ship	Longitude	Reference depth (m)	Maximum velocity (cm s^{-1}) of SIOC	Transports (Sv)		
				at STF	North of STF	South of STF
(a) *Natal*	30°–34°E	2000#–2470#@	NA	NA	32.3	NA
(b) *Natal*	30°–36°E	1390#–3310#@	20.4	65.0	−11.8	NA
(c) *Discovery*	32°–37°E	400#–2120#	32.9	1.5	60.5	NA
(d) *Discovery*	31°–45°E	850#–3310@	29.2	12.8	70.4	0.5
(e) *Conrad*	31°–57°E	700#–3410@	22.3	30.5	35.8	−0.1
(f) *Discovery*	31°–56°E	2440–3280@	17.3	11.7	44.0	8.6
(g) *Africana*	35°–47°E	960#–2110#	20.2	60.1	−5.4	−5.6
(h) *Fuji*	42°–51°E	1850#–2110#	23.9	58.1	−23.7	13.4
(i) *Vema*	42°–46°E	1790#–1950#	2.8	8.5	NA	9.0
(j) *Africana*	55°–58°E	1930#–2380#	5.0	NA	9.6	NA
(k) *Unknown F*	58°–67°E	1900#–2800	13.8	26.1	−57.1	16.5
(l) *Korolev*	64°–65°E	1120#–1590#	7.0	NA	13.2	NA
(m) *Korolev*	64°–65°E	1500#–1720#	NA	NA	−16.0	NA
(n) *Anton Bruun*	64°–65°E	1740#–1970#	3.9	NA	12.6	NA
(o) *Schokalsky*	65°E	1320#–1730#	16.3	25.9	−4.3	5.2
(p) *Schokalsky*	65°E	1120#–1780#	7.7	6.2	14.5	4.3
(q) *Schokalsky*	65°E	1310#–1740#	16.6	21.0	32.4	11.5
(r) *Voeikov*	65°E	790#–1570#	10.5	17.8	4.5	8.1
(s) *Voeikov*	65°E	1500#–1550#	NA	NA	−9.3	NA
(t) *Ob*	66°–70°E	890#–2000	8.2	10.8	2.3	29.3*
(u) *Shirshov*	70°E	410#–540#	NC	NC	NC	NC
(v) *Shirshov*	70°E	1620#–2080#	20.4	31.2	−11.4	7.9
(w) *Anton Bruun*	75°E	1280#–1970#	9.6	18.2	7.4	NA
(x) *Eltanin*	80°–88°E	1960#–2350#	8.4	20.9	−7.5	17.9
(y) *Ob*	97°E	1010#–2610	4.2	4.6	−3.4	−0.3
(z1) *Eltanin*	93°–98°E	3000–3040@	2.8	−0.3	4.4	NA
(z2) *Di amantina*	100°E	810#–2810@	15.6	NA	22.8	NA
(z3) *Di amantina*	102°E	770#–2940@	3.8	1.0	8.8	NA
(z4) *Di amantina*	110°E	2910–3080@	−2.3	−10.4	−0.1	NA
(z5) *Eltanin*	110°–111°E	900#–2970@	−1.3	−5.3	NA	7.4
(z6) *Voekov*	112°–115°E	1240#–1600#	3.4	4.5	−13.5	−5.5
(z7) *Ob*	110°–115°E	670#–1750#	3.7	7.9	−6.1	−11.3

@ Reference depth σ_4 = 45.87 kg m^{-3}.
# Deepest depth available.
* 430-km station spacing.
NA—not available.
NC—not computed.

such compensating transports as in section (b) are not included in Table 2. The 5.4 Sv westward transport in section (g) (R/V *Africana*) is small compared to the 60.1 Sv transported eastward at the STF. Section (h) shows 23.7 Sv to the west in the two station pairs north of the STF, indicating some westward return flow. The 57.1 Sv to the west in section (k) seems unrealistically large and is expected to be due to some data problem. The sections near 65°E show different flow directions north of the front. While section (m) indicates a westward return flow, the westward transports in Table 2 for sections (o) and (s) are compensated by eastward transports of the same amount to the north. Also the westward transports in sections (v), (x), and (y) are compensated mostly by eastward transports of the same amount to the east. Therefore, most of the westward transports are small compared to the eastward flow at the front or are compensated by eastward flow (which is not listed in Table 2) north of the westward flow.

In Wyrtki's (1971) map of the 0–3000-db transport function, a westward transport north of the STF is found at 55°–65°E and east of 80°E. This westward transport must be due to transports in deeper layers, as Wyrtki's maps for 0, 100, and 300 dbar do not show the westward transport. In the data used here, the maximum westward velocity is found between the surface and 100-m depth and is not comparable to the deeper transport in Wyrtki's findings. At 64°–65°E a westward transport near 40°S was found in three out of eight sections (Table 2), and at 66°–102°E again three out

of eight sections show westward transport just north of the STF. This frequency of less than 50% is too small to discuss a westward flow as a permanent feature, but these findings, as well as the maps of Wyrtki (1971), indicate that the region north of the STF is of high variability in flow direction and needs further investigation.

Figure 4 gives an example of the velocity distribution at 65°E for the section done by R/V *Schokalsky* in July 1970 [section (p)]. The speed is less than in the west, but the current north of the STF reaches to 750 m with a speed of more than 6 cm s^{-1}. A second, stronger eastward current can be observed to the south of 43°S. This is the northernmost current band of the Antarctic Circumpolar Current, which is related to the subantarctic front (SAF). The signature of the SAF is not as clear in the thermal field. Sievers and Emery (1978) described the SAF as being associated with enhanced subsurface horizontal temperature gradients between the 3° and 5°C isotherms. Normally between the current band at the SAF and the one at the STF a stagnation region with small velocities can be found, which Peterson and Whitworth (1989) described as the subantarctic zone.

It is at about 60°–90°E that the two current bands at the SAF and the STF come closer together, and the best chance for some water exchange between these currents would exist here. In Geosat satellite altimetry (Chelton et al. 1990) it is observed that large sea level variations appear in the south Indian Ocean near 40°S, 80°E, which indicate large variability in this region. Also, the first empirical orthogonal function (EOF) of sea level variability from these Geosat data indicate an approach of the two currents in this region. Even in satellite-tracked drifter data (Piola et al. 1987; Fig. 1) a confluence of the northern drifters with the southern drifters in the ACC can be observed east of 60°E. For a closer look at the interesting question of a possible water exchange between the two currents near 80°E it would be necessary to have sections where small station spacing was available. For the sections used here, the station spacings were too large with up to 430 km [section (t)]. The larger eastward transport in some sections just south of the STF (Table 2) are all due to a station pair with a large distance between the two stations.

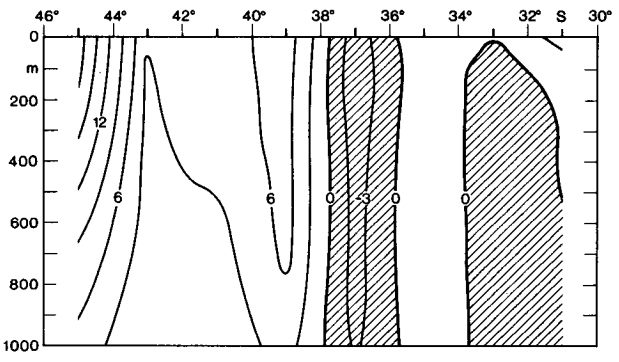

FIG. 4. Vertical distribution of eastward geostrophic speed in centimeters per second (westward flow is shaded) in the upper 1000 m relative to the isopycnal surface σ_2 = 36.94 kg m^{-3} along the south (left)–north (right) line of stations occupied by R/V *Schokalsky* at 65°E in July 1970a [see Table 1, section (p)].

Shown in Fig. 5 is a schematic presentation of the flow field in the upper 1000 m of the southern Indian Ocean derived from the transport distribution of all sections except for the section (u), done by *Shirshov* at 70°E, where data were collected only for the upper 500 m. Because of the inhomogeneous dataset from the period 1934–1974 and the variability in the transport rates, this figure should only be regarded as a schematic flow field from the available data. The current band at the STF continues through the entire south Indian Ocean. This current band reaches depths of about 1000 m and is therefore not only a surface drift. It also shows a current core and is distinct from the ACC; therefore, it has to be regarded as a current and is named here South Indian Ocean Current (SIOC). Below 1000-m depth the velocities decrease quickly, and the surface to 1000-m transport seems to be a good representation of the SIOC.

In the west, where the Agulhas Return Current becomes the SIOC, the mean geostrophic transports in the upper 1000 m are on the order of 60 Sv, in agreement with the 54 and 65 Sv computed by Bennett (1988). When reaching the Southwest Indian Ridge near 50°E, about 20 Sv recirculate and the SIOC reduces to 40 Sv. Another 20 Sv return to the north at about 65°E above the eastern side of the Crozet Basin and 20 Sv remain as the SIOC between 65°E and 90°E and cross the shallow Southeast Indian Ridge. The computed transports including the transports in the north of the sections, which are not included in Table 2 in case of a reversal in flow direction north of the STF, indicate a mainly northwestward direction of the northward flowing water. But as transports are quite variable near 60°E, such a northwestward return flow needs more data to be proven. East of 90°E the SIOC splits with 10 Sv flowing north between 90° and 100°E and 10 Sv flowing to the northwest toward the Australian continent and into the Perth Abyssal Plain region. This flow separates from the STF at about 100°E. The northern band of the ACC is only partly included in the sections used here but is included in Fig. 5, where transport rates are available. The sections were chosen to cross the region of the STF, but not to cross the ACC. For complete transport estimates of the ACC, longer sections and a different reference layer for the ACC would be necessary, but this was not the aim of this study.

The flow of the SIOC in Fig. 5 is not shown to continue into the South Australia Basin south of Australia. The sections at and east of 110°E show quite variable tranports near the STF, which did not indicate a permanent flow in an eastly or westly direction at the STF.

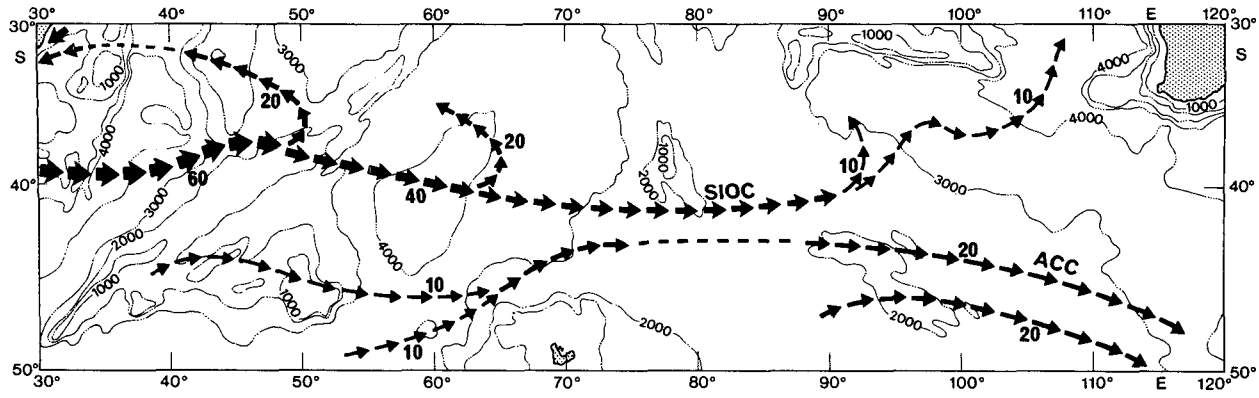

FIG. 5. Schematic illustration of the flow field in the south Indian Ocean. The flow of the South Indian Ocean Current (SIOC) and of the northern part of the Antarctic Circumpolar Current (ACC) are shown by arrows. Note that the main portion of the transport of the ACC is not resolved by the data used here. The transports for the upper 1000 m in Sverdrup is given by the numbers. The main features of the topography are included as thin lines with depth isolines in 1000-m steps.

Instead, the northeastward flow, east of 100°E, seems to be the normal path of the waters of the SIOC, as both zonal sections used at about 32°S showed a northward transport in the order of 10 Sv in the upper 1000 m at about 108°E. Also mean temperature–salinity relationships around Australia (Ridgway and Loch 1987) indicate that most of the subtropical water of the Indian Ocean does not flow into the Great Australian Bight south of Australia. The water in the area south of Australia appears to have formed on the continental shelf and to sink off the continental shelf edge (Ridgway and Loch 1987).

It is unlikely that the subtropical water from the SIOC flows farther eastward south of Australia, as Tasmania builds up a barrier for the flow. Harris et al. (1987) investigated the seasonal variability in the water masses at Tasmania. They found that subtropical water rarely extended as far South as Tasman Island in summer and subantarctic water never extended as far north as Flinders Island. Therefore, the subtropical water would have to flow eastward north of Tasmania into the shelf sea of the Bass Strait. There an outflow exists with seasonal variations of Bass Strait water into the western Tasman Sea, but a quantitative estimate of the seasonal variation does not exist (Tomczak and Tanner 1989). Results from some drift bottle experiments (Newell 1961) have led to the belief that in the Bass Strait the net flow during winter is toward the east, while currents are weak or westward during summer (Tomczak 1987). Therefore, a permanent flow of the water of the SIOC south of Australia is unlikely, and most of the subtropical water of the Indian Ocean recirculates in the Indian Ocean.

4. Summary

In this paper we have looked into the distribution of the subtropical front in the southern Indian Ocean and the current associated with the front. The investigation of the front did not give new information with regard to the local distribution of the front. The new information is on the current related to the front.

The current associated with the STF is typically at the surface front and closes the circulation of the south Indian Ocean subtropical gyre in the south. South of the STF is a region of weak flow that separates the southern limb of the subtropical gyre, called here the South Indian Ocean Current, from the northern bands of the Antarctic Circumpolar Current at the SAF. At depths of 800–1000 m, the SIOC is still recognizable as enhanced current core, so it is more than just a surface drift.

The SIOC southeast of South Africa has a volume transport that averages about 60 Sv in the upper 1000 m. Its transport diminishes to about 10 Sv southwest of Australia. Compared with the South Atlantic Current (SAC) in the south Atlantic, the transport of the SIOC is stronger in the formation region on the western side but loses more water on the way east and is smaller than the transport of the SAC on the eastern side.

One open question is how the water moving north recirculates. The findings here show that the return flow integrated between 0 and 1000 m gets a northwestward component already south of 30°S except east of 100°E (Fig. 5). This would be in good agreement to the isolines in dynamic height anomaly 0–1000 and 0–2500 dbar in Gordon and Molinelli (1982) and the bimonthly figures of geopotential topography 300 relative to 1000 dbar in Wyrtki (1971). On the other side the mean flow field of the surface drifters (Piola et al. 1987) and drift card experiments described in South African investigational reports (unpublished) indicate a circulation cell extending most of the way between Africa and Australia. From Wyrtki's (1971) maps of geopotential topography for different depths, it can be concluded that the near surface water influenced by the strong winds in the Southern Ocean moves mainly to the east while the water at 100-m depths or below

has a large tendency to move north and northwest in the western and central Indian Ocean.

More data with smaller station spacing are needed to investigate details of the SIOC, such as the width of the current or the influence of the topography, and to collect a database large enough to investigate a possible seasonal variability or the water exchange with the ACC. Nevertheless, it is clear that the South Indian Ocean Current exists and that it closes the circulation of the south Indian Ocean subtropical gyre in the south. As the SIOC shows a lot of similarities with the South Atlantic Current described by Stramma and Peterson (1990), the interesting question comes up, whether there is also a distinct current north of the ACC in the much wider South Pacific Ocean. The surface distribution of salinity in the Pacific (Gordon and Molinelli 1982) shows in three of the four seasons in which data were available, a twisted distribution of the isohalines and a northward shift of the isohalines in the eastern South Pacific for the region of the STF. This leads one to believe that the situation in the Pacific might be different and more complicated than in the Indian and Atlantic oceans, although the geopotential anomaly of the sea surface in the Pacific (Reid 1986) indicates a weak flow near 40°S.

Acknowledgments. This work has been supported by the Deutsche Forschungsgemeinschaft in Bonn, Federal Republic of Germany. I thank M. Tomczak for helpful discussions, B. A. Warren for historical background information, G. Longman for checking the manuscript, and A. Eisele for drafting. The data from the WODC were made available with the help of the German Data Center. I would like to acknowledge the work of all ship crews and scientists who collect hydrographic data and make them available to the oceanographic community through the data centers.

REFERENCES

Bennett, S. L., 1988: Where three oceans meet: The Agulhas Retroflection region. Ph.D. dissertation, Woods Hole Oceanographic Institution/Massachusetts Institute of Technology Joint Program in Oceanography, 367 pp.

Chelton, D. B., M. G. Schlax, D. L. Witter, and J. G. Richman, 1990: Geosat altimeter observations of the surface circulation of the Southern Ocean. *J. Geophys. Res.*, **95,** 17 877–17 903.

Cresswell, G. R., T. J. Golding, and F. M. Boland, 1978: A buoy and ship examination of the subtropical convergence south of western Australia. *J. Phys. Oceanogr.*, **8,** 315–320.

Deacon, G. E. R., 1933: A general account of the hydrology of the south Atlantic Ocean. *Discovery Reports,* **7,** 171–238.

——, 1937: The hydrology of the Southern Ocean. *Discovery Reports,* **15,** 3–122.

Dietrich, G., K. Kalle, W. Krauss, and G. Siedler, 1980: General Oceanography. An Introduction, 2d ed. J. Wiley, 626 pp.

Edwards, R. J., and W. J. Emery, 1982: Australasian Southern Ocean frontal structure during summer 1976–77. *Aust. J. Mar. Freshwater Res.*, **33,** 3–22.

Emery, W. J., and J. Meincke 1986: Global water masses: Summary and review. *Oceanol. Acta.*, **9,** 383–391.

Findlay, A. G., 1866: A Directory for the Navigation of the Indian Ocean. Richard Holmes Laurie, 113 pp.

Gordon, A. L., and E. J. Molinelli, 1982: Southern Ocean Atlas: Thermohaline and Chemical Distributions. Columbia University Press, 11 pp.

Harris, G., C. Nilsson, L. Clementson, and D. Thomas, 1987: The water masses of the east coast of Tasmania: Seasonal and interannual variability and the influence of phytoplankton biomass and productivity. *Aust. J. Mar. Freshwater Res.*, **38,** 569–590.

Lutjeharms, J. R. E., 1989: The role of mesoscale turbulence in the Agulhas Current system. Mesoscale/Synoptic Coherent Structures in Geophysical Turbulence, Proc. of the 20th Int. Liege Colloq. on Ocean Hydrodynamics, J. H. C. Nihoul and B. M. Jamart, Eds., Elsevier Oceanography Series, **50,** Amsterdam, 357–372.

——, and R. C. Van Ballegooyen, 1988: The retroflection of the Agulhas Current. *J. Phys. Oceanogr.*, **18,** 1570–1583.

Montgomery, R. B., 1958: Water characteristics of the Atlantic and world oceans. *Deep-Sea Res.*, **5,** 134–148.

Newell, B. S., 1961: Hydrology of south-east Australian waters. CSIRO Division of Fisheries and Oceanography Tech. Paper, **10,** 22 pp.

Peterson, R. G., and T. Whitworth III, 1989: The Subantarctic and Polar fronts in relation to deep water masses through the southwestern Atlantic. *J. Geophys. Res.*, **94,** 10 817–10 838.

——, and L. Stramma, 1991: Upper-level circulation in the South Atlantic Ocean. *Progress in Oceanography,* Vol. 26, Pergamon 1–73.

Piola, A. R., H. A. Figueroa, and A. A. Bianchi, 1987: Some aspects of the surface circulation south of 20°S revealed by First GARP Global Experiment drifters. *J. Geophys. Res.*, **92,** 5101–5114.

Reid, J. L., 1981: On the mid-depth circulation of the World Ocean. Evolution of Physical Oceanography. B. A. Warren and C. Wunsch, Eds., MIT Press, 70–111.

——, 1986: On the total geostrophic circulation of the South Pacific Ocean. Flow pattern, tracers and transports. *Progress in Oceanography,* Vol. 16, Pergamon 1–61.

Ridgway, K. R., and R. G. Loch, 1987: Mean temperature-salinity relationships in Australian Waters and their use in water mass analysis. *Aust. J. Mar. Freshwater Res.*, **38,** 553–567.

Sievers, H. A., and W. J. Emery, 1978: Variability of the Antarctic polar frontal zone in Drake Passage—summer 1976–1977. *J. Geophys. Res.*, **83,** 3010–3022.

Stramma, L., and R. G. Peterson, 1989: Geostrophic transport in the Benguela Current region. *J. Phys. Oceanogr.*, **19,** 1440–1448.

——, and ——, 1990: The South Atlantic Current. *J. Phys. Oceanogr.*, **20,** 846–859.

Tchernia, P., 1980: Descriptive Regional Oceanography. Pergamon Mar. Ser., Vol. **3,** Pergamon Press, 253 pp.

Tomczak, M., 1987: The Bass Strait Water during summer 1981–1982. *Contin. Shelf Res.*, **7,** 561–572.

——, and E. Tanner, 1989: An estimate of Bass Strait water movement in the western Tasman Sea during the Austral Coastal Experiment. *Aust. J. Mar. Freshwater Res.*, **40,** 465–469.

Warren, B. A., 1981: Deep circulation of the World Ocean. Evolution of Physical Oceanography. B. A. Warren and C. Wunsch, Eds., MIT Press, 6–41.

Wyrtki, K., 1971: Oceanographic Atlas of the International Indian Ocean Expedition. Nat. Sci. Found., Washington, D.C., 531 pp.